Conditional-Mean Estimation Via Jump-Diffusion Processes in Multiple Target Tracking/Recognition *

M. I. Miller[†] and A. Srivastava[†] and U. Grenander[‡]

Abstract

A new algorithm is presented for generating the conditional mean estimates of functions of target positions, orientation and type in recognition and tracking of an unknown number of targets and target types. Taking a Bayesian approach a posterior measure is defined on the tracking/target parameter space by combining the narrowband sensor array manifold model with a high resolution imaging model, and a prior based on airplane dynamics. The Newtonian force equations governing rigid body dynamics are utilized to form the prior density on airplane motion. The conditional mean estimates are generated using a random sampling algorithm based on *Jump-Diffusion* processes, [1], for empirically generating MMSE estimates of functions of these random target positions, orientations and type under the posterior measure. Results are presented on target tracking and identification from an implementation of the algorithm on a networked Silicon Graphics and DECmpp/MasPar parallel machines.

*Submitted to the *IEEE Transactions on Signal Processing*. This paper was presented in part at the 29th Annual Allerton Conference on Communication, Control and Computing, 1991, University of Illinois at Urbana-Champaign, Illinois, and at the Communications and Informations Sciences and Systems Conference at Johns Hopkins University, March 1993. This work was supported by the ARO DAAL03-92-G-0141, ONR N00014-92-J-1418, ONR N00014-94-1-0859, and Rome Laboratory F30602-92-C-0004 to Michael I. Miller and ARO/MIT DAAL03-92-G-0115, ONR N00014-91-J-1021, ARL MDA972-93-1-0012, and NSF DMS-9217655 to Ulf Grenander.

[†]Department of Electrical Engineering, Electronic Signals and Systems Research Laboratory, Washington University St. Louis, MO. 63130

[‡]Division of Applied Mathematics, Brown University, Providence, Rhode Island

1 Introduction

This paper focuses on automated tracking and recognition of objects in remotely sensed complex dynamically changing scenes. Grenander's global shape models are used herein, extended to parametric representations of arbitrary and unknown model order, in which typical shape is represented via templates, with variability represented via transformation groups applied to the templates. The types of variability associated with the classical geometry are accommodated via the *Euclidean groups* involving both the rigid motions of translation and rotation. Since the objects are under dynamic motion, *the parameter spaces involves Cartesian products of these similarity groups.*

The second fundamental type of variability is associated with the model order (parametric dimension) and model type (recognition). In any scene there may be variable numbers of and different kinds of targets existing in the scenes for varying periods of time, implying the target number and therefore parametric dimension are unknown apriori. *Hence, the inference or hypothesis space becomes a search across countable disconnected unions of these Cartesian product groups*, with the model order and model type a variable to be inferred. We take a Bayesian approach, i.e. we define a prior distribution supported on this countable union of spaces, from which the posterior distribution is constructed. The parametric representation of the target scene is selected to correspond to *conditional expectations* under this posterior.

As we are particularly interested in non-cooperative moving targets, the algorithms are made robust to motion by incorporation of knowledge about motion dynamics into the prior distribution. The Newtonian force equations, a system of differential equations governing the motion of targets are used to induce the prior. These differential equations are parameterized by the target and or sensor type, and its orientation motion described by rotations in the special orthogonal group $SO(3)$ of 3×3 orthogonal matrices with determinant 1. It is the introduction

of these Newtonian force equations which makes tracking and recognition inseparable, since the equations of motion are explicitly parameterized by the sequence of airplane orientations. This provides the significant link between tracking algorithms based on data from narrowband sensors arrays in which the target is unresolved in the data (effectively a point), and high resolution information perhaps provided by a second sensor preserving the orientation information from which target recognition is performed. In part, it is this fundamental link which has motivated us to solve the tracking/recognition problem in a single consistent estimation framework in which the inference proceeds via the fusion of multi-sensor data: in our case, a *narrowband sensor array output* and *high-resolution images*.

Concerning the generation of conditional expectations, except under the most simplifying set of assumptions, the posterior distribution will be highly nonlinear in the parameters of hypothesis space, thus, precluding the direct closed form analytic generation of conditional expectations. Towards this end we have taken advantage of the explosion which has occurred over the past 10 years in the statistics community on the introduction of random sampling methods for the empirical generation of estimates from complicated distributions; see for example the reviews [2, 3]. Motivated by such approaches, we have previously described a new family of random sampling algorithms [4, 1] for generating conditional expectations in such disconnected hypothesis spaces. The random samples are generated via the direct simulation of a Markov process whose state moves through the hypothesis space with the *ergodic property* that the transition distribution of the Markov process converges to the posterior distribution. This allows for the empirical generation of conditional expectations under the posterior. To accommodate the connected and disconnected nature of the state spaces, the Markov process is forced to satisfy *jump-diffusion dynamics*. i.e. through the connected parts of the parameter space (Lie manifolds) the algorithm searches continuously, with sample paths corresponding to solutions of

standard diffusion equations; across the disconnected parts of parameter space the jump process determines the dynamics. The infinitesimal properties of these jump-diffusion processes are selected so that various sample statistics converge to their expectation under the posterior.

The original motivation for introducing jump-diffusions in [4, 1] is to accommodate the very different continuous and discrete components of the object discovery process. Given a conformation associated with a target type, or group of targets, the problem is to identify the orientation and translation parameters accommodating the variability manifest in the viewing of each object type. For this, the parameter space is sampled using diffusion search in which the state vector winds continuously through the similarities following gradients of the posterior. The second distinct part of the sampling process corresponds to the target type and number deduction during which the target types are being discovered, with some subset of the scene only partially "recognized" at any particular time during the process. The second type of change in parameter space are associated with a set of non-continuous transformations of the scene controlled by the jump process. A jump in hypothesis space corresponds to (i) jumping between different object types, (ii) hypothesizing a new object in the scene or a "change of mind" via the deletion of an object in the scene, or (iii) the merging or splitting of tracks and objects. The jump intensities are governed by the posterior density, with the process visiting configurations of higher probability for longer exponential times, and the diffusion equation governing the dynamics between jumps. It is the fundamental difference between diffusions (almost surely continuous sample paths) and jump processes (making large moves in parameter space in small time) which allows us to explore the very different connected and non-connected nature of hypothesis space.

Now automated target tracking and recognition are well known problems in the signal processing and control system's literature, with a great deal of published work on multiple target

tracking posed as state estimation problems [5, 6, 7]. In such approaches Kalman filter based techniques are emphasized, with linear descriptions of state playing a fundamental role. For situations in which the observed data are non-linear in target parameters the use of the extended Kalman filter has been proposed corresponding to linear approximations which prove valid for particular scenarios. There also now exists a substantial body of important work in tracking the directions of arriving signals from multiple moving sources recorded via sensor arrays [8, 9, 10]. In such sensor array based approaches the non-linear relationship between the parameters of motion and the sensor data are addressed directly, the linear Kalman filter state equations for tracking guiding or providing initial conditions for the gradient based estimators generated from the likelihood. In these non-linear data models, several variations of the gradient based techniques are used to solve the problem in mostly maximum-likelihood settings. However, the majority of researchers utilize simplifying assumptions which are not always valid in a general tracking scenario. For example, targets may be assumed stationary between sample times with multiple (~ 100) snapshots at each sample time, whereas, in general, for a moving target, each data sample reflects a new position. Also, though researchers base their models on simplified versions of target dynamics for the tracking scenario, mostly constant velocity - constant acceleration state constraint equations have been used because of their linear nature. These restricted motions are partly due to assumptions required for Kalman updating, but perhaps more fundamentally due to the separation of the tracking and recognition problems. The more informative priors used in this paper require high resolution recognition as the priors are coupled to the target type and its orientations. In part, this is one of the major results of this work.

In the work presented here, we define a random sampling based solution for generating minimum mean squared error estimates of the state variables for tracking and recognition problems in

a general setting. We assume data from a narrowband sensor array providing azimuth-elevation data for object tracking, and optical or radar imagers providing detailed information about the target-type and orientation. The goal is to track and recognize the unknown number of non-cooperative sources. The paper is organized as follows. In section 2 we define the parameter spaces with the posterior distribution derived in section 3. Section 4 describes an inference algorithm based on jump-diffusion processes and section 5 presents various results.

2 Recognition Via Deformable Templates

We use the global shape models and pattern theoretic approach introduced by Grenander [11, 12] to analyze complex scenes. As the basic building blocks of the hypotheses we define a subset of generators $\mathcal{G}^o$, which contains each target type $a \in \mathcal{A}$ ($\mathcal{A}$ is the alphabet of target types) placed at the origin of the inertial reference frame aligned to the inertial axes. The fundamental variability in target space is accommodated by applying the transformations $T(\phi)$ and $T(p)$ to the templates $g^o \in \mathcal{G}^o$ according to

$$T(\phi) : \begin{bmatrix} x_1 \\ x_2 \\ x_3 \end{bmatrix} \rightarrow \begin{bmatrix} 1 & 0 & 0 \\ 0 & cos\phi_1 & sin\phi_1 \\ 0 & -sin\phi_1 & cos\phi_1 \end{bmatrix} \begin{bmatrix} cos\phi_2 & 0 & -sin\phi_2 \\ 0 & 1 & 0 \\ sin\phi_2 & 0 & cos\phi_2 \end{bmatrix} \times \begin{bmatrix} cos\phi_3 & sin\phi_3 & 0 \\ -sin\phi_3 & cos\phi_3 & 0 \\ 0 & 0 & 1 \end{bmatrix} \begin{bmatrix} x_1 \\ x_2 \\ x_3 \end{bmatrix} \tag{1}$$

$$T(p) : \begin{bmatrix} x_1 \\ x_2 \\ x_3 \end{bmatrix} \rightarrow \begin{bmatrix} x_1 + p_1 \\ x_2 + p_2 \\ x_3 + p_3 \end{bmatrix}, \tag{2}$$

where $\phi \in [0, 2\pi]^3$ with $0, 2\pi$ identified (herein referred to as the 3-dimensional torus $\mathcal{T}(3)$), and $p \in R^3$ is the translation vector. These parameterized transformations operate on the templates from $\mathcal{G}^o$ generating the full set of possible elements constituting any scene. The left panel of Figure 1 shows a rendering of one of the 3-D ideal targets $g^o \in \mathcal{G}^o$ under one such transformation.

The Bayes posterior is parameterized via the set of transformations, as well as the airplane type. A pattern consisting of a single track arises from a single target appearing and disappearing at random times $t_1^{(m)}, t_2^{(m)} \in [t_0, t]$ the observation period, with the m-th track parameter vector $x^{(m)}$ an element of the space $x^{(m)} \in (\mathcal{X}_0 \bigcup \sharp)^{[t_0,t]} \times \mathcal{A}$, $\mathcal{X}_0 \equiv \mathcal{T}(3) \times \Re^3$. The symbol $\sharp$ is used to denote the absence of the target from the scene. It will be useful for us to introduce the notation $x^{(m)}(\tau), \tau \in [t_0, t]$ to denote the set of parameters encoding the m-th target at time τ. An M-track parameter vector $x(M)$ becomes

$$x(M) \in \mathcal{X}_t(M) \equiv \left[\left(\mathcal{X}_0 \bigcup \sharp \right)^{[t_0,t]} \times \mathcal{A} \right]^M . \tag{3}$$

Since the number of the targets M is unknown a priori, the complete parameter space is defined as $\mathcal{X}_t = \bigcup_{M=0}^{\infty} \mathcal{X}_t(M)$. The estimation problem is to estimate the individual configurations as well as the number M.

3 Bayesian Posterior

Minimum mean squared error ($MMSE$) parameter estimates are generated via their empirical computation under the posterior measure. As the posterior is proportional to the product of the prior density and the observed data likelihood we first derive a prior on the parameter space followed by a model for the data generation which determines the posterior. For real

time estimation problems, the posterior density is an explicit function of t denoted $\pi_t(\cdot)$. In the Bayesian approach the estimates are for each time t conditioned on the data observed up to that time t.

3.1 Prior Density on Parameter Space $\mathcal{X}_t$

Airplane dynamics: The formulation of the prior measure on airplane positions is based on equations of motion for rigid bodies. We use an approach, in which the prior is induced via partial differential equations by assuming the forcing function to be a white process, which induces a Gaussian process with covariance corresponding to the differential operator expressing airplane dynamics. For this purpose, we use a formulation of airplane dynamics through differential equations as described by Cutaia and O'Sullivan [13]. Airplane dynamics are most straightforwardly expressed using the velocities projected along the body-fixed axes, called the body-frame velocities and here denoted $v(s) = [v_1(s)\ v_2(s)\ v_3(s)]$. They are depicted in the right panel of Figure 1.

Following standard rigid body analysis (see [14], for example) and neglecting the earth's curvature, motion and wind effects, the translational velocities $v(s)$ and rotational velocities $q(s) = [q_1(s)\ q_2(s)\ q_3(s)]$ satisfy the following set of differential equations:

$$\begin{aligned}
\dot{v}_1(s) - q_3(s)v_2(s) + q_2(s)v_3(s) &= f_1(s)\ , \\
\dot{v}_2(s) + q_3(s)v_1(s) - q_1(s)v_3(s) &= f_2(s)\ , \\
\dot{v}_3(s) - q_2(s)v_1(s) + q_1(s)v_2(s) &= f_3(s)\ , \\
I_1\dot{q}_1(s) - (I_2 - I_3)q_2(s)q_3(s) &= \Gamma_1(s)\ , \\
I_2\dot{q}_2(s) - (I_3 - I_1)q_1(s)q_3(s) &= \Gamma_2(s)\ , \\
I_3\dot{q}_3(s) - (I_1 - I_2)q_2(s)q_1(s) &= \Gamma_3(s)\ ,
\end{aligned} \tag{4}$$

where $[f_1(s)\ f_2(s)\ f_3(s)]$ is the vector of applied translational forces, $[I_1\ I_2\ I_3]$ is the vector of rotational inertias, and $[\Gamma_1(s)\ \Gamma_2(s)\ \Gamma_3(s)]$ is the vector of applied torques. The first three equations describe the airplane's translational motion, while the next three describe its rotational motion.

At this time the prior which we have used for tracking is "somewhat less informative" in that only the first three equations, on translational motion, are used; detailed models of the targets associated with the torques for describing the rotational motion are not yet explicitly incorporated. The system matrix $A(\phi(s), \dot{\phi}(s))$ parameterizing Eqns. 4 is

$$\begin{bmatrix} 0 & -q_3(s) & q_2(s) \\ q_3(s) & 0 & -q_1(s) \\ -q_2(s) & q_1(s) & 0 \end{bmatrix},$$

with the velocities, inertial positions and Euler angles are related using the standard transformation to relate body-frame velocities with inertial frame positions according to

$$p(s) = \int_{t_0}^{s} \Psi(\tau) v(\tau) d\tau + p(t_0), \tag{5}$$

where $p(t_0)$ the initial position is assumed known and $\Psi(\tau)$ is the standard orthogonal rotation matrix given in Eqn. 1 parameterized by the Euler angles $\phi(\tau)$. The rotational motion determines the prior since with reference to the fixed inertial frame the angular velocity projections, $q(s)$, onto the rotating body axes determine the system matrix $A(\phi(s), \dot{\phi}(s))$. The $q(s)$ vectors are none other than the rates of change of the Euler orientation angles according to $q_1 = \dot{\phi_1} - \dot{\phi_3} sin(\phi_2),\ q_2 = \dot{\phi_2} cos(\phi_1) + \dot{\phi_3} cos(\phi_2) sin(\phi_1),\ q_3 = -\dot{\phi_2} sin(\phi_1) + \dot{\phi_3} cos(\phi_2) cos(\phi_1)$.

For the construction of the "informative" part of the prior, first condition the linear dif-

ferential equations on the sequence of system matrices $A(\phi(s), \dot{\phi}(s))$, via conditioning on the sequence of Euler rotation angles. Then the velocity process is a conditional Gaussian process induced by assuming the forcing function on the momentum equation to be a white process of fixed spectral density. The covariance function is derived as follows. Define the state transition matrix $\Phi(\tau, \cdot)$ as the unique solution of the matrix differential equation

$$\frac{dM(s)}{ds} = -A(\phi(s), \dot{\phi}(s))M(s) \ , \quad M(\tau) = I \ , \tag{6}$$

then the covariance of the body frame velocity process becomes

$$\mathcal{K}_v(s_1, s_2) = \sigma \int_{t_0}^{min(s_1,s_2)} \Phi(t_1, s_1)\Phi^{\dagger}(t_1, s_2)dt_1 + \Phi(t_0, s_1)\mathcal{K}_v(t_0, t_0)\Phi^{\dagger}(t_0, s_2) \ , \tag{7}$$

where $\mathcal{K}_v(t_0, t_0)$ is the covariance of the initial velocity, $v(t_0)$. The inertial position process is then Gaussian with covariance $\mathcal{K}_p(s_1, s_2) = \int_{t_0}^{s_1} \int_{t_0}^{s_2} \Psi(\tau_1)\mathcal{K}_v(\tau_1, \tau_2)\Psi^{\dagger}(\tau_2)d\tau_1 d\tau_2$. The covariance function is parameterized by the sequence of airplane orientations thereby demonstrating the fundamental link between tracking unresolved targets and high-resolution recognition algorithms.

The more "diffuse" component of the prior is developed by assuming the Euler angles are fixed for small sampling intervals, giving a sequence of angles $\phi(1), \phi(2), \ldots, \phi(j) = \phi(s), s \in [j\Delta, (j+1)\Delta)$. Then, the marginal on $\phi(j)$ takes the form of a Markov Von-Mises prior on the torus $\mathcal{T}(3)$ (see e.g. [15]) with the density $\prod_{i=1}^{3} \frac{1}{2\pi I_0(\kappa_i)} e^{\kappa_i cos(\phi_i(j) - \bar{\phi}_i(j))}$, where $I_0(\cdot)$ is the modified Bessel function of the first kind and order zero, and $\kappa = [\kappa_1 \ \kappa_2 \ \kappa_3]$ is the vector of concentration parameters, and $\bar{\phi(j)} = [\bar{\phi}_1(j) \ \bar{\phi}_2(j) \ \bar{\phi}_3(j)]$ is the mean of $\phi(j)$. The orientation process is made Markov by assigning the previous state as the mean of the present state, giving

a potential of the form

$$\sum_j \sum_{i=1}^{3} \kappa_i cos(\phi_i(j) - \phi_i(j-1)) \ . \tag{8}$$

Recognition: We want to drive the algorithm towards deductions which are as simple as possible. Therefore, we use priors based on run-length coding to encourage hypotheses with minimal numbers of aggregated tracks. For this, associate with a target appearing at time $t_1^{(m)}$ and exiting at time $t_1^{(m)} + t_2^{(m)}$ the number of bits $log^* t_1^{(m)} + log^* t_2^{(m)} + log|\mathcal{A}| + \frac{6}{2} t_2^{(m)} log(sample - size)$, log^* the iterated logarithm $log + loglog + \ldots$ defined by Rissanen [16, 17] for constructing priors on the reals. Then the *complexity* prior for an M-track scene has potential

$$\left(log^* t_1^{(m)} + log^* t_2^{(m)} + log|\mathcal{A}| + \frac{6}{2} t_2^{(m)} log(sample - size) \right) \ . \tag{9}$$

3.2 Data Likelihood

The likelihood of the collected data correspond to two sensor types, a *tracking sensor* consisting of an array of passive sensors and a range radar, and a *high-resolution imaging* sensor.

Low resolution tracking: As shown in the left panel of Figure 2, for azimuth-elevation coordinate tracking, a cross array of n isotropic sensors is assumed as in [18, 19, 20, 21] using the standard narrowband signal model developed in [22]. Accordingly, depending on the geometry of the sensor arrangement, the phase lags of the signal reaching different sensor elements are known functions of the source locations. The deterministic signal model for sensor arrays is used in which the $n \times 1$ sensor array measurement vector $y_1(\tau)$, $\tau \in [t_0, t]$ is complex Gaussian distributed with diagonal covariance and mean $E\{y_1(\tau)\} = \sum_{m=1}^{\infty} d(x^{(m)}(\tau)) 1_{\mathcal{X}_0}(x^{(m)}(\tau)) s^{(m)}(\tau)$, with $s^{(m)}(\tau)$ the signal amplitude of the m-th track at time τ. Notice the indicator function $1_{\mathcal{X}_0}(x^{(m)}(\tau))$ selects the targets that contribute to the array manifold at time τ, $d(p^{(m)}(\tau))$ is the direction vector determined by the array geometry and the position of the m-th target.

Since the tracking array responds to the inertial positions of the target most naturally in azimuth and elevation, we convert from rectangular coordinates $p(t) = [p_1(t)\ p_2(t)\ p_3(t)] \in R^3$ to polar coordinates, $[r(t)\ \alpha_1(t)\ \alpha_2(t)] \in R^+ \times [0, 2\pi)^2$, (range, elevation and azimuth) using the standard relationship,

$$r = \sqrt{p_x^2 + p_y^2 + p_z^2}\ , \alpha_1 = arctan \frac{p_z}{\sqrt{p_x^2 + p_y^2}}\ , \alpha_2 = arctan \frac{p_y}{p_x}\ . \tag{10}$$

High resolution imaging: While the statistical models for high-resolution radar imaging are being incorporated in this problem by others ([23, 24, 25, 26, 27, 28]), all of the results shown here are based on an optical imaging system as depicted in the right panel of Figure 2. In this system, the data are a sequence of 2-D images resulting from projecting the scene volume containing targets onto the focal plane of the imaging sensor; i.e., the imaging process is modeled as a far field orthographic projection. Since the parameter set $x(M)$ completely determines the imaged volume, the projection is a deterministic operation from the parameter space to the measurement space $\Re^{\mathcal{L}\times[t_0,t]}$, $\mathcal{P} : \mathcal{X}_t \rightarrow \Re^{\mathcal{L}\times[t_0,t]}$, where $\mathcal{L}$ is the 2-D image space. For all of the results shown here the high-resolution imaging data is a non-zero mean white Gaussian process with mean the projective transformation of the scene: $E\{y_2(\tau)\} = \mathcal{P}(x(\tau)), \tau \in [t_0, t]$.

The posterior distribution is obtained as the product of the data likelihood and the prior density and is defined explicitly by Eqns. 11,12 below.

Remark: For observing the range locations of the targets, a range radar is assumed with the observations modeled as normally distributed with mean $|p(\tau)|$, the 2-norm of the position vector at time $\tau \in [t_0, t]$.

4 Random Sampling for Generating Conditional Expectations

4.1 The parameter space.

In particularizing the jump-diffusion algorithm to the multiple tracking problem it will be convenient to suppress explicit dependence on time t. Therefore, for each time t we will have a distribution for which the jump-diffusion process will be constructed. The parameter spaces themselves will be indexed by t, and form an increasing family of spaces.

The crucial part of the problem still remaining is the derivation of the inference algorithm: For all of the possible scenes we assume that the targets are stationary during some fundamental data sampling intervals, with the parameters and sensor data represented by their values on some index set $\{\tau_j\}_{j=1,\ldots,J}$, J the total number of sample points in the observation interval $\tau_j \in [t_0, t]$. Note, J is actually a function of t. Then an M-track parameter vector becomes $x(M) \in \mathcal{X}(M) \equiv (\mathcal{X}_0 \bigcup \{\sharp\})^{MJ} \times \mathcal{A}^M$ with the complete parameter space being $\mathcal{X} = \bigcup_{M=0}^{\infty} \mathcal{X}(M)$. It will be useful to define the number of track segments in the m-th track $n^{(m)}$, and the total number of track-segments as $n(M)$, implying for example, $x(M) \in \mathcal{X}_0^{n(M)} \times \mathcal{A}^M$.

The **posterior** μ is of the Gibb's form with the potential H_M for $x(M) \in \mathcal{X}(M)$ becoming

$$\begin{aligned} H_M(x(M)) \quad = \quad & 1/\sigma_1 \sum_{j=1}^{J} |y_1(\tau_j) - \sum_{m=1}^{M} d(x^{(m)}(\tau_j)) 1_{\mathcal{X}_0}(x^{(m)}(\tau_j))|^2 + 1/\sigma_2 \sum_{j=1}^{J} |y_2(\tau_j) - \mathcal{P}(x(\tau_j))|^2 \\ & + \sum_{m=1}^{M} \left(p^{(m)} K_p^{(m)} p^{(m)} + \sum_{j=2}^{n^{(m)}} \sum_{i=1}^{3} \kappa_i^{(m)} cos(\phi_i^{(m)}(\tau_j) - \phi_i^{(m)}(\tau_{j-1})) \right) \\ & + \sum_{m=1}^{M} \left(log^* n^{(m)} + log^* t_1^{(m)} + log|\mathcal{A}| + \frac{6}{2} t_2^{(m)} log(sample - size) \right) . \end{aligned} \tag{11}$$

The first two quadratic terms are associated with the tracking data and the high resolution imaging data. The last three terms are the prior terms on the tracking parameters, Von-Mises orientations and track complexity, respectively For arbitrary $x \in \mathcal{X}$, define the potential

$H_M(x) = 0$, for $x \notin \mathcal{X}(M)$. Then the posterior measure $\mu(\cdot)$ with density $\pi(\cdot)$ is in Gibb's form according to

$$\mu(dx) = \frac{\sum_{M=0}^{\infty} e^{-H_M(x)} 1_{\mathcal{X}(M)}(x)}{\mathcal{Z}} dx \ , \tag{12}$$

with the normalizer $\mathcal{Z} = \sum_{M=0}^{\infty} \int_{\mathcal{X}(M)} e^{-H_M(x)} dx$.

Now for the development which follows it will be convenient to define the part of the posterior which does not include the prior. This we define as L_M and is given by the formula

$$L_M(x(M)) = 1/\sigma_1 \sum_{j=1}^{J} |y_1(\tau_j) - \sum_{m=1}^{M} d(x^{(m)}(\tau_j)) 1_{\mathcal{X}_0}(x^{(m)}(\tau_j))|^2 + 1/\sigma_2 \sum_{j=1}^{J} |y_2(\tau_j) - \mathcal{P}(x(\tau_j))|^2 \ ,$$

with the prior potential term denoted by

$$\begin{aligned} P_M(x(M)) \quad = \quad & \sum_{m=1}^{M} \left(p^{(m)} K_p^{(m)} p^{(m)} + \sum_{j=2}^{n^{(m)}} \sum_{i=1}^{3} \kappa_i^{(m)} cos(\phi_i^{(m)}(\tau_j) - \phi_i^{(m)}(\tau_{j-1})) \right) \\ & + \sum_{m=1}^{M} \left(log^* n^{(m)} + log^* t_1^{(m)} + log|\mathcal{A}| + \frac{6}{2} t_2^{(m)} log(sample - size) \right) \ . \end{aligned}$$

Remark: Notice, in identifying model M with an M-track configuration the potential must be adjusted so that the m-th track covariance $K_p^{(m)}$ is an $n^{(m)} \times n^{(m)}$ matrix appropriate for the m-th track. We would be more precise by identifying models $(n^{(1)}, n^{(2)}, \ldots n^{(M)}, M)$ with index $k \in \aleph$, from which the potential is then uniquely defined in the usual sense. However, with the subtle breach of notational convention we simply define H_M as the potential associated with an M-track configuration and modify the potential according to the variable numbers of parameters associated with the tracks.

4.2 The basic jump-diffusion set-up.

The crucial part of the problem still remaining is the derivation of the inference algorithm: that is *how shall we carry out hypothesis formation?* We follow the analysis outlined in [4, 1], in which conditional expectations with respect to the posterior density $\pi(\cdot)$ are generated empirically. First identify with each model an index $k \in \aleph$ with parameter space $\mathcal{X}(k)$ of dimension $n(k)$. The full hypothesis space $\mathcal{X} = \cup_{k=0}^{\infty} \mathcal{X}(k)$. The posterior distribution μ is then of the Gibb's type supported on $\mathcal{X}$, i.e. for all set $\mathcal{A} \subset \mathcal{X}$ Lebesgue measurable,

$$\begin{aligned} \mu(\mathcal{A}) &= \sum_{k=0}^{\infty} \mu(\mathcal{A} \cap \mathcal{X}(k)) \ , \\ &= \sum_{k=0}^{\infty} \int_{\mathcal{A} \cap \mathcal{X}(k)} \frac{e^{-H_k(x(k))}}{\mathcal{Z}} dx(k) \ . \end{aligned} \tag{13}$$

The goal is to essentially sample from μ generating a sequence of samples $X(s_1), X(s_2), \ldots$ with the property that

$$1/n \sum_{j=1}^{n} f(X(s_j)) \stackrel{n \to \infty}{\to} \int_{\mathcal{X}} f(x) \mu(dx) \ . \tag{14}$$

This we do via the construction of a Markov process $X(s)$ which satisfies *jump-diffusion dynamics* through $\mathcal{X}$ in the sense that (i) on random exponential times the process jumps from one of the countably infinite set of spaces $\mathcal{X}(k), k = 0, 1, \ldots$ to another, and (ii) between jumps it satisfies diffusions of dimension $n(k)$ appropriate for that space.

The process $X(s)$ within each of the multiple sub-spaces is a diffusion with infinitesimal drifts $a(x(k)) \in R^{n(k)}$ and infinitesimal variance matrix $B(x(k))$, an $n(k) \times n(k)$ matrix. It is the existence of this multiple disconnected union of spaces $\mathcal{X}$ which motivates the introduction of the second transformation type on the models, transformations which act by changing one model type to another with its resulting configuration. The transformations we shall term *simple moves*

which are drawn probabilistically from a family $\mathcal{F}$ of changes in the model types $k \in \aleph$, and are applied discontinuously, with the simple moves defining transitions through $\aleph$, $\mathcal{F} : \aleph \to \aleph$. The family of transitions are chosen large enough to act transitively in the sense that given any pair $k', k'' \in \aleph$ it should be possible to find a finite chain of transitions that leads from k' to k''.

The set $\mathcal{F}$ controls the jump dynamics in the jump-diffusion processes as follows. The jump process corresponds to movement from one subspace to another on the jump times with transition probability measure $Q(x, dy) = \frac{q(x,dy)}{q(x)}$, $\int_{\mathcal{X}} Q(x, dy) = 1$. The measures $q(x, dy)$ are defined in the standard way [29]: $q(x, dy) = \lim_{\epsilon \to 0} \frac{1}{\epsilon} \Big(\Pr\{X(s+\epsilon) \in dy | X(s) = x\} - 1_{dy}(x) \Big)$, with $q(x) = \int_{\mathcal{X} \backslash x} q(x, dy)$. The set $\mathcal{F}$ determines which measures are non-zero.

As we have shown for purely Euclidean spaces [4, 1], the proper choice of jump transition measures and diffusion drifts and variances (stochastic gradients) will make μ on $\mathcal{X}$ invariant with ergodic averages generated from the process converging to their expectations. See theorem 1 of [1].

4.2.1 The jump process.

The **jump process** is controlled by the family of changes $\mathcal{F}$ which control the movement through the non-connected subspaces. Changes in model type will include increasing and decreasing track length, increasing and decreasing number of tracks, and changing the target types. The set of transformations are defined as $\mathcal{F} = \{\vartheta^d_{t(j)}, \vartheta^d_{s(j)}, \vartheta^b_{t(j)}, \vartheta^b_{s(j)}, \vartheta_{a(j)}\}$. The first two correspond to deletion or removal of the j-th track and segment, which are mappings $\vartheta^d_{t(j)} : \mathcal{X}_0^{n(M)} \times \mathcal{A}^M \to \mathcal{X}_0^{n(M)-1} \times \mathcal{A}^{M-1}$, $\vartheta^d_{s(j)} : \mathcal{X}_0^{n(M)} \times \mathcal{A}^M \to \mathcal{X}_0^{n(M)-1} \times \mathcal{A}^M$, respectively. The second two are birth operators birthing tracks and segments to the j-th place or track, and are mappings $\vartheta^b_{t(j)} : \mathcal{X}_0^{n(M)} \times \mathcal{A}^M \to \mathcal{X}_0^{n(M)+1} \times \mathcal{A}^{M+1}$, $\vartheta^b_{s(j)} : \mathcal{X}_0^{n(M)} \times \mathcal{A}^M \to \mathcal{X}_0^{n(M)+1} \times \mathcal{A}^M$, respectively. The last operator simply changes the target type, $\vartheta_{a(j)} : \mathcal{X}_0^{n(M)} \times \mathcal{A}^M \to \mathcal{X}_0^{n(M)} \times \mathcal{A}^M$. It should

be noted that the addition of only unit length tracks is allowed, and unit length track segments, as well as deletions of only unit length tracks or segments. Define the set, of indices of tracks in $x(M)$ which are candidates for deletion, by $\{m : 1 \leq m \leq M, n^{(m)} = 1\}$ and let $M_1(x(M))$ be the cardinality of this set. For the increments in parameter space, an explicit notation denoting a specific segment or track added to the configuration will be needed. Let $\oplus_j$ stand for the addition of track segments or tracks to the existing configuration, i.e. $x(M) \oplus_j y(1)$ represents an $M+1$ track configuration formed by adding $y(1)$ to $x(M)$ at the j-th location in the list, and $x(M) \oplus_j y$ signifies addition of a segment to the j-th track of $x(M)$.

These are the only transformations of model type that are allowed. To carry the evolution of the state forward from the diffusion we make the jump measures singular with respect to the Lebesgue measures in the respective subspaces which the jump transformations move into. For this, the part of the state which is not being added or deleted remains unchanged after the jump transformation. This corresponds to the following transition measures of the type,

$$
\begin{aligned}
q(x(M), dy(M+1)) &= \sum_{j=1}^{M+1} q_t^b(x(M), y(M+1)) \delta_{x(M)} \Big(d(\vartheta^d_{t^{(j)}} y(M+1)) \Big) dy(1) \,, \\
q(x(M), dy(M)) &= \sum_{j=1}^{M} q_s^b(x(M), y(M)) \delta_{x(M)} \Big(d\Big(\vartheta^d_{s^{(j)}} y(M) \Big) \Big) dy \\
&+ \sum_{j=1}^{M} q_s^d(x(M), y(M)) \delta_{\vartheta^d_{s^{(j)}} x(M)}(dy(M)) \,, \\
&+ \sum_{j=1}^{M} q_a(x(M), y(M)) \delta_{x(M)} \Big(d\Big(\vartheta_{a^{(j)}} y(M) \Big) \Big) \,, \\
q(x(M), dy(M-1)) &= \sum_{j=1}^{M} q_t^d(x(M), y(M-1)) \delta_{\vartheta^d_{t^{(j)}} x(M)}(dy(M-1))
\end{aligned} \tag{15}
$$

Let $\mathcal{F}^1(x(M)) \subset \aleph$ be the set of models that can be reached from $x(M)$ in one jump move, and $\mathcal{X}(\mathcal{F}^1(x(M)))$ the space containing the configurations of these types. The total jump

intensity becomes

$$q(x(M)) = \int_{\mathcal{X}(\mathcal{F}^1(x(M)))} q(x(M), dy) \, . \tag{16}$$

4.2.2 The diffusion process.

The **diffusion process** between jumps controls the dynamics of $X(s)$ in their respective sub-spaces. For the sub-space associated with M tracks having $n(M)$ segments the diffusion flows through the manifold $\mathcal{X}_0^{n(M)} = \mathcal{T}(3)^{n(M)} \times R^{3n(M)}$ associated with the orientations $\phi \in \mathcal{T}(3)$ and positions $p \in R^3$. The restriction of a previous result in Theorem 1 from [1] to Euclidean spaces unfortunately prevents its direct application to the tracking problem in which the torus is involved. Even the most innocuous appearing stochastic differential equation (S.D.E.) make little sense when the manifold is curved in any way. This forces us to use more general results on Lie manifolds as described in [30] and adapted to the tracking case as follows.

Associate with the first $3n(M)$ components of the state vector the flow through $\mathcal{T}(3)^{n(M)}$, and the last $3n(M)$ components the flow through $R^{3n(M)}$ according to $X(s) = [X_1(s), X_2(s)]$, $X_1(s) \in \mathcal{T}(3)^{n(M)}$, $X_2(s) \in R^{3n(M)}$. Also, define $\frac{e^{-P(y(1)|x(M))}}{Z_T(1)}$, $\frac{e^{-P_j(y|x(M))}}{Z_S(1)}$ as the conditional prior densities on the single track and single segment spaces given the current configuration $x(M)$, respectively, with $Z_T(1), Z_S(1)$ being their normalizers. P_j denotes the attachment of the segment y to the j^{th}-track of the set $x(M)$. Then we have the following theorem.

Theorem 1 *IF the jump diffusion process $X(s)$ has the properties that*

1. *the diffusion $X(s)$ within any of the subspaces $\mathcal{X}_0^{n(M)}$ satisfies the S.D.E.*

$$X_1(s) = \left[X_1(0) + \int_0^s -\frac{1}{2} \nabla_1 H_M(X(\tau)) d\tau + W_1(s) \right]_{\text{mod } 2\pi} , \tag{17}$$

$$X_2(s) = X_2(0) + \int_0^s -\frac{1}{2} \nabla_2 H_M(X(\tau)) d\tau + W_2(s) \, , \tag{18}$$

where $[\cdot]_{\mathrm{mod}\ 2\pi}$ *is taken componentwise,* ∇_1, ∇_2 *are the gradients with respect to the orientation and position (velocity) vectors respectively, and* $W_1(s), W_2(s)$ *are standard vector Wiener processes of dimensions* $3n(M)$*,*

2. *and the birth/death parameters of the jump measures*

$$
\begin{aligned}
q_t^b(x(M), x(M) \oplus_j y(1)) &= \frac{1}{5(M+1)} e^{-[L_{M+1}(x(M)\oplus_j y(1)) - L_M(x(M))]_+} \frac{e^{-P(y(1)|x(M))}}{Z_T(1)}, \quad j = 1, .., M+1 \ , \\
q_s^b(x(M), x(M) \oplus_j y) &= \frac{1}{5M} e^{-[L_M(x(M)\oplus_j y) - L_M(x(M))]_+} \frac{e^{-P_j(y|x(M))}}{Z_S(1)}, \quad j = 1, .., M \ , \\
q_t^d(x(M), \vartheta^d_{t(j)} x(M)) &= \frac{1}{5M_1(x(M))} \frac{e^{-[L_{M-1}(\vartheta^d_{t(j)} x(M)) - L_M(x(M))]_+}}{Z_T(1)} 1_{\{m>0\}}(M_1(x(M)) \ , \\
& \qquad\qquad j \in \{m : 1 \le m \le M, n^{(m)} = 1\} \ , \\
q_s^d(x(M), \vartheta^d_{s(j)} x(M)) &= \frac{1}{5M} \frac{e^{-[L_M(\vartheta^d_{s(j)} x(M)) - L_M(x(M))]_+}}{Z_S(1)} \ , \quad j = 1, .., M \ , \\
q_a(x(M), \vartheta_{a(j)} x(M)) &= \frac{1}{5M} e^{-[L_M(\vartheta_{a(j)} x(M)) - L_M(x(M))]_+}, \quad j = 1, .., M \quad . \qquad (19)
\end{aligned}
$$

THEN, $X(s_j)$ *converges in variation norm to* μ*.*

Proof: The proof follows the general approach in [1, 30] with details summarized for this problem in the Appendix.

4.3 Algorithm Implementation

The jump-diffusion process satisfying Theorem 1 is constructed as follows. Initialize with $t_0 = 0, i = 0$.

1. Generate an exponential random variable u with mean 1.

2. For $s \in [s_i, s_i + u)$, $X(s)$ follows the stochastic differential Eqns. 17,18 in subspace determined by $X(s_i)$.

3. On random time $s_{i+1} = s_i + u$, define $x_{\text{old}} = X(s_{i+1}^-)$ and determine $M = M_{\text{old}}$ of x_{old} the number of tracks in $X(s_{i+1}^-)$.

4. Draw one of the 5 possible jump choices from the set $\{t^b, s^b, t^d, s^d, a\}$ according to the distribution $\{\frac{1/5}{Z}, \frac{1/5}{Z}, \frac{1/5 Z_T(1)}{Z} 1_{\{m>0\}}(M_1(x_{old})), \frac{1/5 Z_S(1)}{Z}, \frac{1/5}{Z}\}$, with $Z = \frac{1}{5} + \frac{1}{5} Z_T(1) 1_{\{m>0\}}(M_1(x_{old})) + \frac{1}{5} Z_S(1) + \frac{1}{5} + \frac{1}{5}$.

   If, t^b, then draw a 1-length track $y(1)$ from a uniform prior on $\mathcal{X}_0 \times \mathcal{A}$ and draw $j \in \{1, 2, \ldots, M+1\}$ uniformly:

$$x_{\text{new}} \leftarrow x_{\text{old}} \oplus_j y(1) \ .$$

   Else If, t^d, draw $j \in \{m : 1 \leq m \leq M, n^{(m)} = 1\}$ uniformly:

$$x_{new} \leftarrow \vartheta^d_{t(j)} x_{\text{old}} \ .$$

   Else If, s^b, then draw $j \in \{1, 2, \ldots, M\}$ uniformly and draw $y \in \mathcal{X}_0$ from the Von-Mises prior on $\mathcal{T}(3)$ and the Gaussian prior on $\Re^3$, $\frac{e^{-P_j(y|x(M))}}{Z_S(1)}$, conditioned on the current j^{th} track configuration:

$$x_{new} \leftarrow x_{\text{old}} \oplus_j y \ .$$

   Else If, s^d, draw $j \in \{1, 2, \ldots, M\}$ uniformly:

$$x_{new} \leftarrow \vartheta^d_{s(j)} x_{\text{old}} \ .$$

   Else, Draw $j \in \{1, 2, \ldots, M\}$ uniformly:

$$x_{new} \leftarrow \vartheta_{a(j)} x_{\text{old}} \ .$$

5. Determine M_{new} of x_{new}.

6. If, $L_{M_{\text{old}}}(x_{\text{old}})) - L_{M_{\text{new}}}(x_{\text{new}}) > 0$, $X(s_{i+1}) \leftarrow x_{\text{new}}$

   Else $X(s_{i+1}) \leftarrow x_{\text{new}}$ with probability $e^{-[L_{M_{\text{new}}}(x_{\text{new}}) - L_{M_{\text{old}}}(x_{\text{old}})]}$ and

   Else $X(s_{i+1}) \leftarrow x_{\text{old}}$ with probability $1 - e^{-[L_{M_{\text{new}}}(x_{\text{new}}) - L_{M_{\text{old}}}(x_{\text{old}})]}$.

7. $i \leftarrow i + 1$, return to 1.

Since a track-segment of length 1 correspond to $y \in \mathcal{X}_0$ consisting of the position and orientation components, the discretized form of Eqn. 4 is used for the position and the Markov Von-Mises prior on the torus $\mathcal{T}(3)$ used for the orientation component. The candidates for deletion are obtained by removing the last segment from the current j^{th} track estimate or the j^{th} track estimate itself.

5 Results

Below we focus on single track identification in 3-D space; see [31] for multiple target tracking in 2-D.

For the implementation of the jump-diffusion algorithm for estimating the motion of a single target, i.e. M = 1, the parameter space becomes $\mathcal{X}_0^{[t_0,t]} \times \mathcal{A}$. For the implementation there are a total of two target types, $\mathcal{A} \equiv \{1, 2\}$. The algorithm was jointly implemented using the *flight simulator* software on the Silicon Graphics workstation for generating the data sets, and a massively parallel 4096 processor SIMD DECmpp/MasPar machine for implementing the tracking-recognition algorithm. Figure 4 shows the simulation environment for a sample target-flight observed by sensor systems located on ground represented by the mesh. The target motion is observed at 1500 times during the flight.

The array geometry corresponds to a 64-element cross-array of isotropic sensors located at

half-wavelength spacing. The tracking data $\{y_1(\tau), \tau \in [t_0, t)\}$ is a 64-element complex vector with mean $d(p(\tau))s(\tau)$ and additive complex Gaussian white noise of the Goodman's class. The direction vector corresponds to the array takes the form

$$[e^{-\frac{i31}{2}\lambda_1(\tau)},\ e^{-\frac{i29}{2}\lambda_1(\tau)}\ ,...,e^{\frac{i31}{2}\lambda_1(\tau)},\ e^{-\frac{i31}{2}\lambda_2(\tau)},e^{-\frac{i29}{2}\lambda_2(\tau)}\ ,..,\ e^{\frac{i31}{2}\lambda_2(\tau)}]^T\ ,\quad i=\sqrt{-1}\ ,$$

where $\lambda_1(\tau) = \pi cos(\alpha_1(\tau))sin(\alpha_2(\tau))$, and $\lambda_2(\tau) = \pi cos(\alpha_1(\tau))sin(\alpha_2(\tau))$, $\alpha_1(\tau), \alpha_2(\tau)$ is the azimuth, elevation angles of the target position $p(\tau)$. Since we use the velocity representation the azimuth and elevations are generated using the standard coordinate transformation of Eqns. 5,10. The upper panels in Figure 3 display the azimuth-elevation power spectra of the tracking data, generated by projecting the data vector onto the candidate direction vectors, for two target locations.

The 2-D imaging data $\{y_2(\tau), \tau \in [t_0, t)\}$ consists of 4096 Gaussian random variables associated with a 64×64 imaging lattice. The mean is $\mathcal{P}(x(t))$ where $\mathcal{P}(\cdot)$ is simply the 2-D projection of the rendered object positioned and oriented at $p(\tau), \phi(\tau)$, with additive noise. The lower panels in Figure 3 show two data samples obtained by high resolution imaging of the target along its flight.

At any given time t the jump-diffusion algorithm is run to generate samples from the posterior distribution generated by the data up to time t. This simulation is performed until the next data set arrives at $t + 1$ when the algorithm starts sampling from the new posterior. For sampling the jump-diffusion Markov process is constructed as follows. For the single object case the possible jump transformations through parameter space involve either addition of a track segment $y \in \mathcal{X}_0$, deletion of a track segment, or a change of target type. The set of changes

$\mathcal{F} \equiv \{\vartheta^d_{s(1)}, \vartheta^b_{s(1)}, \vartheta_{a(1)}\}$ are transformations of the type

$$x(1) \in \mathcal{X}_0^{n(1)} \times \mathcal{A} \quad \rightarrow \quad x(1) \oplus_1 y \in \mathcal{X}_0^{n(1)+1} \times \mathcal{A} \ , \tag{20}$$

$$x(1) \in \mathcal{X}_0^{n(1)} \times \mathcal{A} \quad \rightarrow \quad \vartheta^d_{s(1)} x(1) \in \mathcal{X}_0^{n(1)-1} \times \mathcal{A} \ , \tag{21}$$

$$x(1) \in \mathcal{X}_0^{n(1)} \times \mathcal{A} \quad \rightarrow \quad \vartheta_{a(1)} x(1) \in \mathcal{X}_0^{n(1)} \times \mathcal{A} \ . \tag{22}$$

Shown in Figure 4 is the evolution of the random sampling algorithm for estimating the target track. The grey track represents the true airplane path, consisting of 1500 track segments, used in data generation with the estimated track shown overlapping in black at three different times during the estimation. Figure 5 shows a magnified view of a section of the track, formed of 8 track-segments, being estimated by the jump-diffusion algorithm. The top 4 panels illustrate the jump part of the algorithm for which we have turned off the diffusion. These upper panels shows successive guesses of the jump process which continually attempt to add and delete new track segments. Since the actual object has created a path which is longer then that which has been inferred by the algorithm during the early segments, the jump process always chooses to add new track segments. Notice, that on each addition the new segment is drawn from the prior on flight dynamics, which are parameterized by the track up to that point in time. Hence, the jump algorithm tends to infer track segments which are close to the true track if the current state vector is close to it. Because the diffusion has been turned off, notice the disparity between the track and the state of the algorithm.

The lower panels show the result of applying the diffusion to the state vector. The flow of the panels corresponds to increasing simulation time as the diffusion simulates from the posterior with the state brought into alignment.

Figure 6 depicts the importance of the dynamics based prior. Based on the equations of

motion and the track history the candidate segments are generated and accepted/rejected according to their likelihood. To show the support of the prior distribution in "phase space", the upper panels plot the 10 highest prior probability candidates placed at the track end for the algorithm to choose from. Each panel corresponds to a different time during the inference. The top row shows that if the track vector is close to the true track, the cone of candidates predicts well the future position. The lower panel shows the effect of the track state deviating from the true path, where the cone of prediction is not close to the future airplane position.

Figure 7 demonstrates the global importance of the prior distribution in estimating a portion of the target path. The algorithm was run with and without the prior measure, under the same parameters, with the results shown in the figure. The upper panels show the sequence of estimates obtained from the algorithm without any information from airplane dynamics. The lower panels use the prior information based on the equations of motion describing the airplane flight.

6 Acknowledgments

We would like to thank Robert Teichman for a great deal of help in the recognition component of the algorithm. We owe special thanks to Professor Yali Amit who provided the detailed development for the diffusion on Lie groups of which the torus is a particular example.

7 Appendix

Proof of Theorem 2: The proof has two parts: (i) showing that π is an invariant density of the process, and (ii) verifying that the process is irreducible and therefore π is the unique invariant density. Part (ii) follows directly that in [30] using the properties of the jump process and the

fact that the diffusions are each irreducible over their respective subspaces. In part (i) we need to verify the stationarity for both the jump and diffusion components of the Markov process. The generator, or backward Kolmogoroff operator, for the jump-diffusion process (denote it as $A = A^d + A^j$ (diffusion+jump)) characterizes the stationary density in that $\pi(x)$ is stationary for the jump-diffusion if and only if

$$\int Af(x)\pi(x)dx = 0 \tag{23}$$

for all f in the domain of A, $\mathcal{D}(A)$.

The diffusion process has two components corresponding to the S.D.E. on the multi-dimensional torus (17) and the S.D.E. on the Euclidean space of target positions (velocities) (18). To prove invariance of $\pi(x)$ for the diffusion on the torus we use results from [30] on invariant distributions of S.D.E.'s on manifolds, in particular the multi-dimensional torus. To demonstrate the approach, we prove the stationarity condition for the Euclidean component only. Define a set of functions which forms the domain of the generator A as

$$\mathcal{D}(A) = \{f : f = \sum_{M=0}^{K} 1_{\mathcal{X}(M)} f_M, f_M \in \hat{C}^2(\mathcal{X}(M)), K \geq 0\} \ , \tag{24}$$

with $\hat{C}^2$ twice continuously differentiable functions vanishing at ∞. Then the infinitesimal generator for diffusion A^d acting on such a function, $f = \sum_{M=0}^{K} 1_{\mathcal{X}(M)} f_M$, according to Eqn. 23 gives

$$\begin{aligned} \int_{\mathcal{X}} A^d f(x)\pi(x)dx \quad = \quad & \sum_{M=0}^{K} [- \int_{\mathcal{X}(M)} \frac{1}{2} < \nabla H_M(x), \nabla f_M(x) > \frac{e^{-H_M(x)}}{\mathcal{Z}} dx \\ & + \int_{\mathcal{X}(M)} \frac{1}{2} \left(\sum_{i=1}^{3n(M)} \frac{\partial^2 f_M(x)}{\partial p_i^2} \right) \frac{e^{-H_M(x))}}{\mathcal{Z}} dx \ ]. \end{aligned}$$

where $< \cdot, \cdot >$ stands for the vector dot-product and the gradients $\nabla H_M(x), \nabla f_M(x)$ are w.r.t the position (velocity) vector, an element of $R^{3n(M)}$. Integration by parts of the second term, with the fact that the functions f_M vanish at the boundary, results in a term which is negative of the first term. Therefore the given posterior π is the stationary density of the diffusion process.

We note that the curved nature of the torus requires the argument to be modified in sufficiently subtle ways. For details of such modifications to the manifolds associated with Lie groups see [30]. The jump part of the generator A^j is given by

$$A^j f(x) = q(x) \int_{\mathcal{X}(\mathcal{F}^1(x))} Q(x, dy)(f(y) - f(x)) \ ,$$

and computing the adjoint corresponding to the Eqn. 23 (see [1] for illustration) provdes the balance condition

$$q(x)\pi(x)dx = \int_{\mathcal{X}(\mathcal{F}^{-1}(x))} q(y, dx)\pi(y)dy \ , \tag{25}$$

where $\mathcal{F}^{-1}(x) \subset \aleph$ is the subset of models which can reach x in one jump transition. The jump parameters must satisfy Eqn. 25 for the density $\pi(x)$ to be stationary for the jump part of the process. For definiteness, assume $x \in \mathcal{X}(M)$ so that $x \equiv x(M)$ is an M-track configuration. Substituting for the transition measures from Eqns. 15 gives

$$\begin{aligned}
\pi(x(M))dx(M) \quad & [\quad \sum_{j=1}^{M} \int_{\mathcal{X}_0} q_s^b(x(M), x(M) \oplus_j y)dy + \sum_{j=1}^{M} q_s^d(x(M), \vartheta_{s(j)} x(M)) \\
& + \quad \sum_{j=1}^{M+1} \int_{\mathcal{X}_0 \times \mathcal{A}} q_t^b(x(M), x(M) \oplus_j y(1))dy(1) + \sum_{j=1}^{M} q_t^d(x(M), \vartheta_{t(j)} x(M)) \\
& + \quad \sum_{j=1}^{M} q_a(x(M), \vartheta_{a(j)} x(M)) \ ] \\
= dx(M) \ [& \sum_{j=1}^{M} \int_{\mathcal{X}_0} q_s^d(x(M) \oplus_j y, x(M))\pi(x(M) \oplus_j y)dy + \sum_{j=1}^{M} q_s^b(\vartheta_{s(j)} x(M), x(M))\pi(\vartheta_{s(j)} x(M))
\end{aligned}$$

$$+\sum_{j=1}^{M+1}\int_{\mathcal{X}_0\times\mathcal{A}} q_t^d(x(M)\oplus_j y(1),x(M))\pi(x(M)\oplus_j y(1))dy(1)+\sum_{j=1}^{M} q_t^b(\vartheta_{t(j)}x(M),x(M))\pi(\vartheta_{t(j)}x(M))$$
$$+\sum_{j=1}^{M} q_a(\vartheta_{a(j)}x(M),x(M))\pi(\vartheta_{a(j)}x(M))\ ]\ .$$

We will prove this equality treating only the first two summation terms from both sides, corresponding to the birth/death of track-segments; the treatment for the rest being similar. The jump moves considered here, birth/death of track-segments, are defined by Eqns. 20 and 21. Substituting the values for q_s^b, q_s^d from Eqn. 19,

L.H.S.:

$$\begin{aligned}
&\pi(x(M))\ \frac{dx(M)}{Z_S(1)}\ \frac{1}{5M}\ \sum_{j=1}^{M}\ [\ \int_{\mathcal{X}_0} e^{-[L_M(x(M)\oplus_j y)-L_M(x(M))]_+}e^{-P_j(y|x(M))}dy \\
&\qquad\qquad +e^{-[L_M(\vartheta_{s(j)}x(M))-L_M(x(M))]_+}\ ] \\
=\ &\frac{dx(M)}{(\mathcal{Z})(Z_S(1))}\ \frac{1}{5(M)}\ \sum_{j=1}^{M}\ [\ \int_{\Omega_>} e^{-L_M(x(M))}e^{-P_M(x(M))}e^{-P_j(y|x(M))}dy \\
&\qquad\qquad +\int_{\Omega_\leq} e^{-L_M(x(M)\oplus_j y)}e^{-P_M(x(M))}e^{-P_j(y|x(M))}dy \\
&\qquad\qquad +e^{-L_M(x(M))}e^{-P_M(x(M))}e^{-[L_M(\vartheta_{s(j)}x(M))-L_M(x(M))]_+}\ ]\ . \qquad (26)
\end{aligned}$$

R.H.S.:

$$\begin{aligned}
&\frac{dx(M)}{Z_S(1)}\ \frac{1}{5(M)}\ \sum_{j=1}^{M}\ [\ \int_{\mathcal{X}_0} e^{-[L_M(x(M))-L_M(x(M)\oplus_j y)]_+}\pi(x(M)\oplus_j y)dy \\
&\quad +e^{-[L_M(x(M))-L_M(\vartheta_{s(j)}x(M))]_+}e^{-P_j(y|\vartheta_{s(j)}x(M))}\pi(\vartheta_{s(j)}x(M))\ ] \\
=\ &\frac{dx(M)}{(\mathcal{Z})(Z_T(1))}\ \frac{1}{5M}\ \sum_{j=1}^{M}\ [\ \int_{\Omega_>} e^{-L_M(x(M))}e^{-P_M(x(M)\oplus_j y)}dy \\
&\quad +\int_{\Omega_\leq} e^{-L_M(x(M)\oplus_j y)}\ e^{-P_M(x(M)\oplus_j y)}dy \\
&\quad +e^{-[L_M(x(M))-L_M(\vartheta_{s(j)}x(M))]_+}e^{-P_j(y|\vartheta_{s(j)}x(M))}e^{-L_M(\vartheta_{s(j)}x(M))}e^{-P_M(\vartheta_{t(j)}x(M))}\ ]\ , \qquad (27)
\end{aligned}$$

where

$$\Omega_{>} = \mathcal{X}_0 \bigcap \{y : L_M(x(M)) > L_M(x(M) \oplus_j y)\}$$

$$\Omega_{\leq} = \mathcal{X}_0 \bigcap \{y : L_M(x(M)) \leq L_M(x(M) \oplus_j y)\} \ .$$

Comparing Eqns. 26, 27 and combining the prior terms (i.e. $P_M(x(M) \oplus_j y) = P_M(x(M)) + P_j(y|x(M))$, and $P_M(x(M)) = P_M(\vartheta_{s(j)} x(M)) + P_j(y|\vartheta_{s(j)} x(M)))$, the equality is verified.

Q.E.D

References

[1] U. Grenander and M. I. Miller. Representations of knowledge in complex systems. *Journal of the Royal Statistical Society B*, 56(3):549–603, 1994.

[2] B. Gidas. Metropolis type monte-carlo simulation algorithms and simulated annealing. In *Trends of Contemporary Probability*, 1993. to appear.

[3] J. Besag and P. J. Green. Spatial statistics and bayesian computation. *J. Royal Statistical Society B*, 55:25–38, 1993.

[4] U. Grenander and M. I. Miller. Jump-diffusion processes for abduction and recognition of biological shapes. *Monograph of the Electronic Signals and Systems Research Laboratory*, 1991.

[5] Y. Bar-Shalom and E. Tse. Tracking in cluttered environment with probabilistic data association. *Automatica*, (11):451–460, 1975.

[6] Y. Bar-Shalom and T. E. Fortmann. *Tracking and Data Association*. Academic Press, 1988.

[7] Editor: Y. Bar-Shalom. *Multitarget-Multisensor Tracking*. Artech House, 1990.

[8] C. R. Rao, C. R. Sastry, and B. Zhou. Tracking the direction of arrival of multiple moving targets. *IEEE Transactions on Acoustics,Speech and Signal Processing*, accepted for publication, 1993.

[9] C. R. Sastry, E. W. Kamen, and M. Simaan. An efficient algorithm for tracking angles of arrival of moving targets. *IEEE Transactions on Acoustics,Speech and Signal Processing*, ASSP-39(No.1):242–246, 1991.

[10] C. K. Sword, M. Simaan, and E. W. Kamen. Multiple target angle tracking using using sensor array outputs. *IEEE Trans. AES.*, 26(2):367–373, 1990.

[11] W. Freiberger and U. Grenander. Computer generated image algebras. *Internation Federation Information Processing*, 68:1397–1404, 1969.

[12] U. Grenander. Advances in pattern theory: The 1985 Rietz lecture. *The Annals of Statistics*, 17:1–30, 1985.

[13] Nicholas Cutaia and Joseph A. O'Sullivan. Automatic target recognition algorithms using kinematic priors. *Electronic Signals and Systems Research Lab. Monograph*, 1994.

[14] Bernard Friedland. *Control System Design : An Introduction To State-Space Methods.* McGraw-Hill Book Company, 1986.

[15] K.V. Mardia. *Statistics of Directional Data.* Academic Press, London and New York, 1972.

[16] J. Rissanen. A universal prior for integers and estimation by minimum description length. *The Annals of Statistics*, 11:416–431, 1983.

[17] J. Rissanen. Stochastic complexity and modeling. *The Annals of Statistics*, 14, no.3:1080–1100, 1986.

[18] M.I. Miller and D. R. Fuhrmann. Maximum likelihood narrow-band direction finding and the EM algorithm. *IEEE Acoust. Speech and Signal Processing*, 38, No.9:560–577, 1990.

[19] A. Srivastava, M.I. Miller, and U. Grenander. Jump-diffusion processes for object tracking and direction finding. In *Proceedings of the 29th Annual Allerton Conference on Communication, Control and Computing*, pages 563–570, Urbana, Champaign, 1991. University of Illinois.

[20] A. Srivastava, N. Cutaia, M.I. Miller, J. A. O'Sullivan, and D. L. Snyder. Multi-target narrowband direction finding and tracking based on motion dynamics. In *Proceedings of the 30th Annual Allerton Conference on Communication, Control and Computing*, Urbana, Champaign, 1992. University of Illinois.

[21] M.I. Miller, R. S. Teichman, A. Srivastava, J.A. O'Sullivan, and D. L. Snyder. Jump-diffusion processes for automated tracking-target recognition. In *Proceedings of the Twenty-Seventh Annual Conference Conference on Information Sciences and Systems*, pages 617–622, Baltimore, Maryland, March 24-26 1993. Johns Hopkins University.

[22] R. Schmidt. *A signal subspace approach to multiple emitter location and spectral estimation.* Ph.D. Dissertation of Stanford University, Palo Alto, CA., Nov. 1981.

[23] D.L. Snyder, J.A. O'Sullivan, and M.I. Miller. The use of maximum-likelihood estimation for forming images of diffuse radar-targets. In *Transactions of SPIE in Advanced Architectures and Algorithms*, San Diego, California, 1987.

[24] D.L. Snyder, J.A. O'Sullivan, and M.I. Miller. The use of maximum-likelihood estimation for forming images of diffuse radar-targets from delay-doppler data. *IEEE Transactions on Information Theory*, 35(3):536–548, 1989.

[25] J.A. O'Sullivan, P. Moulin, and D.L. Snyder. Cramer-rao bounds for constrained spectrum estimation with application to a problem in radar imaging. In *Proceedings 26th Allerton Conference on Communication, Control, and Computing*, Champaigne, Urbana, October 1988. Urbana, IL.

[26] M.I. Miller, D.R. Fuhrmann, J.A. O'Sullivan, and D.L. Snyder. Maximum-likelihood methods for toeplitz covariance estimation and radar imaging. In Simon Haykin, editor, *Advances in Spectrum Estimation*, pages 145–172. Prentice-Hall, 1990.

[27] P. Moulin, J.A. O'Sullivan, and D.L. Snyder. A method of sieves for multiresolution spectrum estimation and radar imaging. *IEEE Transactions on Information Theory*, 1992.

[28] J.A. O'Sullivan, K. C. Du, R. S. Teichman, M.I. Miller, D.L. Snyder, and V.C. Vannicola. Radar target recognition using shape models. In *Proc. 30th Annual Allerton Conference on Communication,Control, and Computing*, pages 515–523, Urbana, Il., 1992. University of Illinois.

[29] I. I. Gihman and A. V. Skorohod. *Introduction to the Theory of Random Processes*. Saunders, Philadelphia, 1965.

[30] Y. Amit and M.I. Miller. Ergodic properties of jump-diffusion processes. *Monograph of the Electronic Signals and Systems Research Laboratory*, January 1993.

[31] A. Srivastava, M.I. Miller, and U. Grenander. Multi-target direction of arrival tracking. *IEEE Transactions on Signal Processing*, to appear, May 1995.

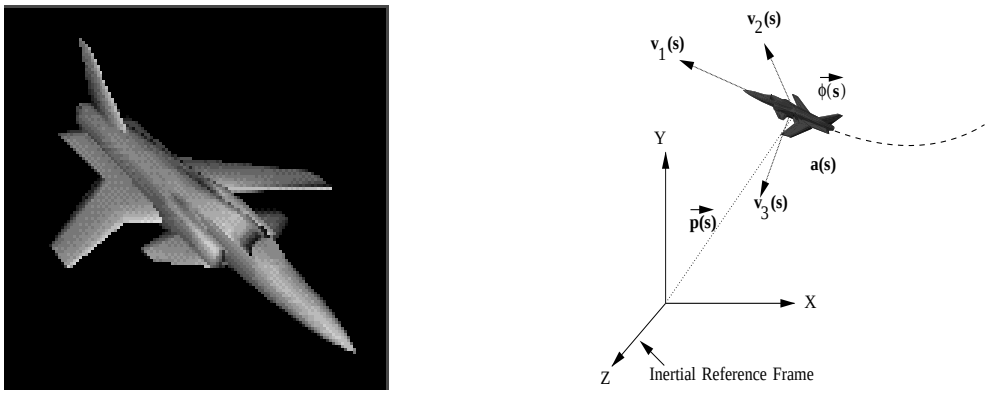

Figure 1: The left panel shows the 3-D target generator $g \in \mathcal{G}^o$ under a similarity transformations. The right panel shows the target located at position $p(s)$, oriented at $\phi(s)$ with velocities $v(s)$ resolved in the body frame coordinates.

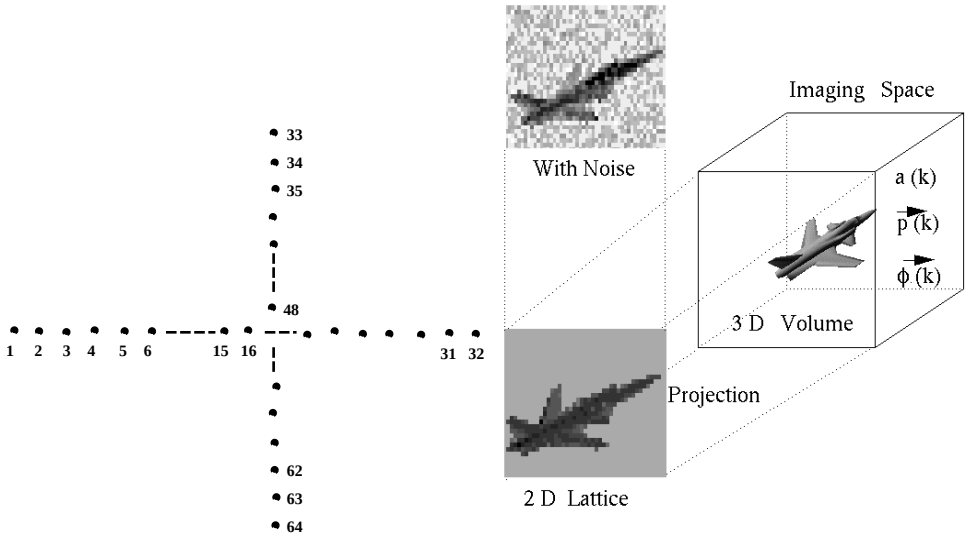

Figure 2: The left panel displays the cross array of isotropic sensors at half wavelength spacing, used to observe the angular location of the target. The right panel shows the far-field orthographic imaging system used for observing the targets at a high resolution.

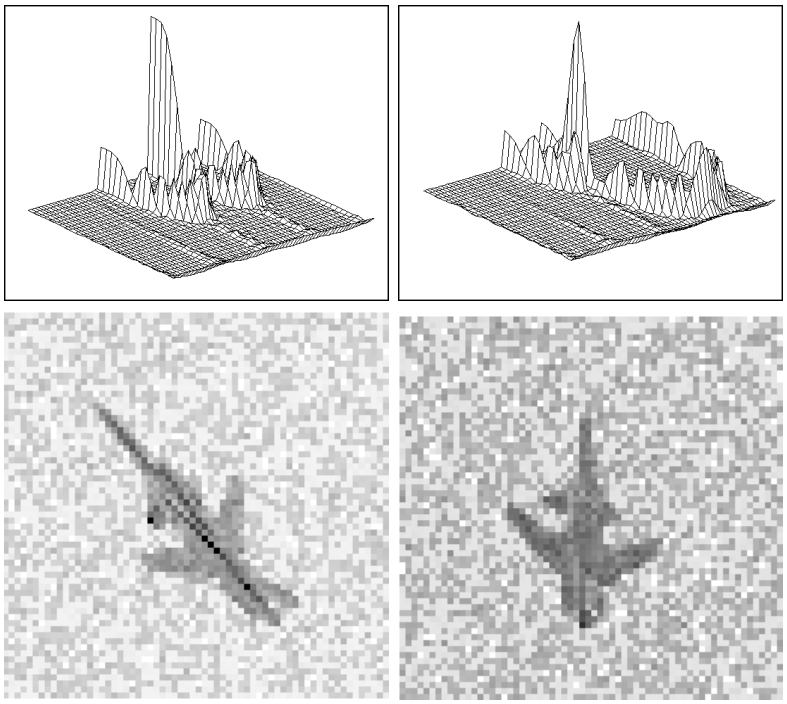

Figure 3: The upper panels show the azimuth-elevation power spectrum of the tracking data at two sample times. The lower panels display the high resolution data sets for the target at two different times during the flight path.

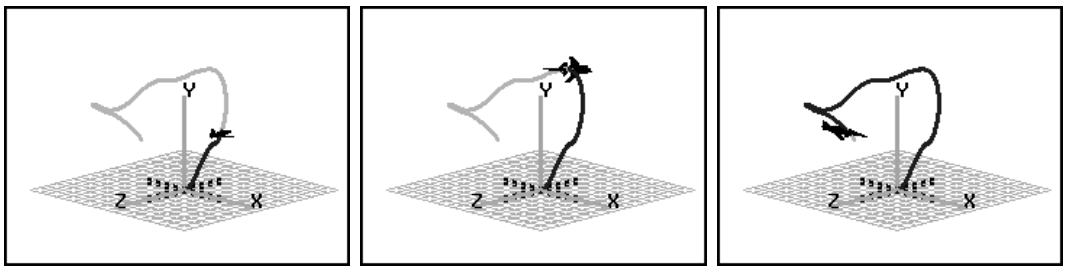

Figure 4: The actual track drawn in grey is observed by the ground based observation system. The track estimates are drawn overlapping in black at three stages of the algorithm.

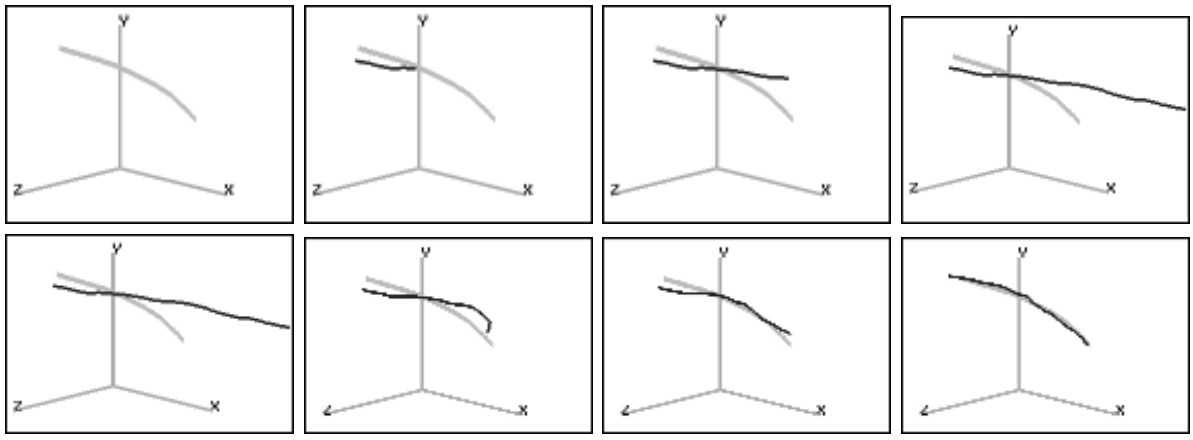

Figure 5: The upper panels show the sequence of jump moves adding segments to the estimated state from left to right, with the diffusion turned off. The lower panels show the continuous diffusion transformation aligning the estimated to the true track via the gradients on the posterior energy.

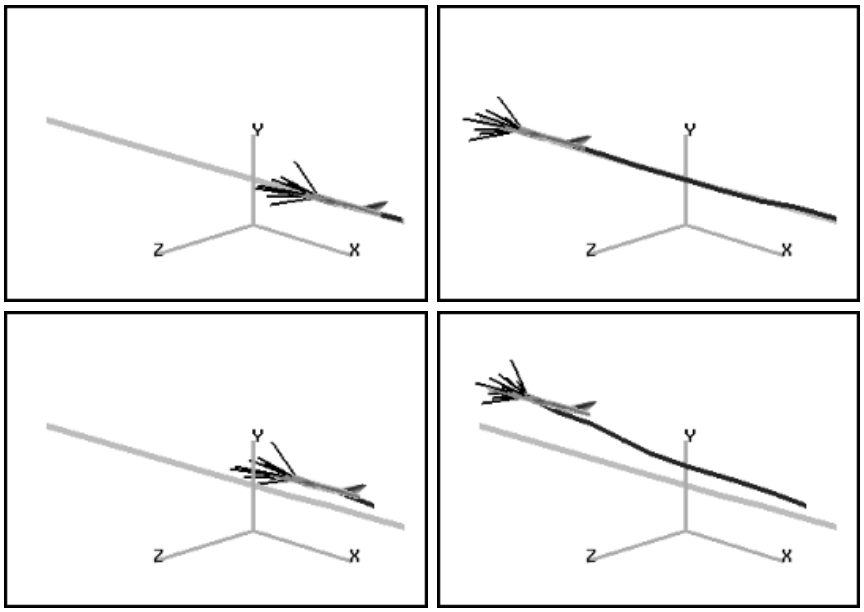

Figure 6: The four panels show candidates from the prior distribution for target path estimation with the high prior probability candidates forming a cone at track end for the algorithm to sample from. The upper panels show the prior with the diffusion on track parameters turned on; the lower panels have the diffusion turned off.

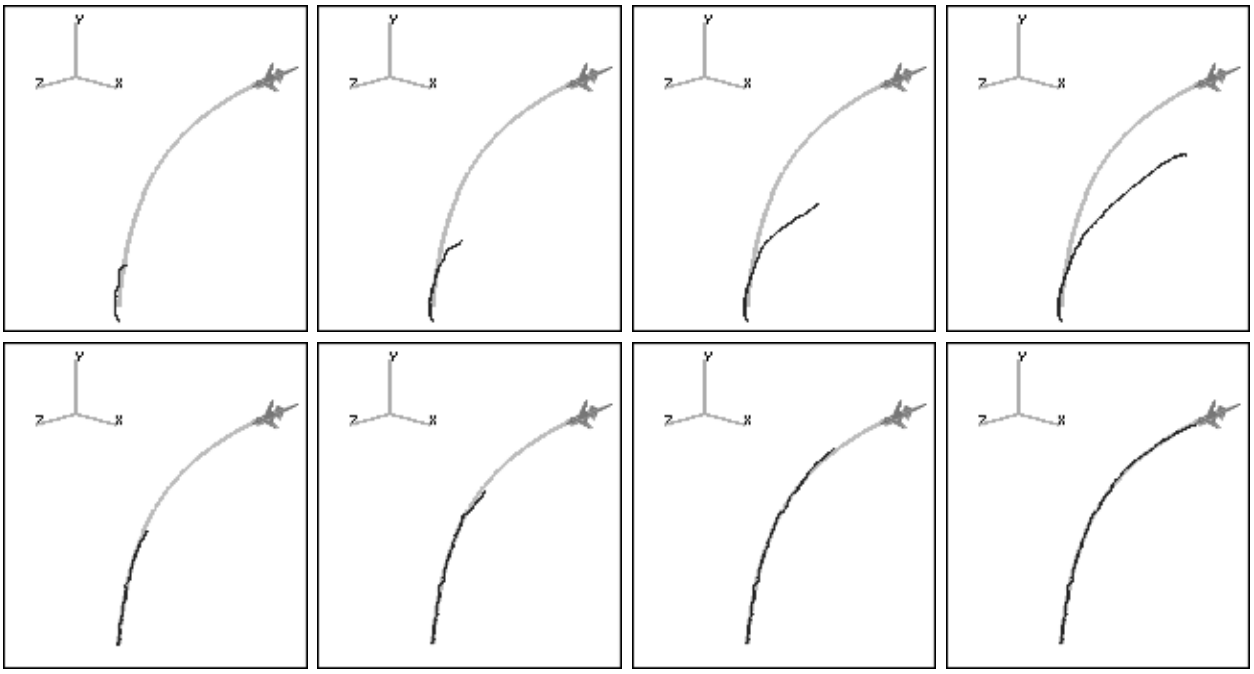

Figure 7: The upper panels display the estimated states at four times without the tracking prior information. The lower panels show the results of the dynamics based estimation algorithm with the prior included.